Available online at www.sciencedirect.com
SCIENCE DIRECT®

ELSEVIER

Geomorphology 55 (2003) 235–247

GEOMORPHOLOGY

www.elsevier.com/locate/geomorph

Post-Oligocene river incision, southern Sierra Madre Occidental, Mexico

David R. Montgomery[a,*], Jorge López-Blanco[b]

[a] Department of Earth and Space Sciences, University of Washington, Seattle, WA 98195, USA
[b] Instituto de Geografia, UNAM, Circuito Ext., Cd. Universitaria, Mexico, 04510 D.F., Mexico

Received 2 November 2001; received in revised form 13 May 2002; accepted 10 March 2003

Abstract

The Sierra Madre Occidental of western Mexico consists of a granitic basement covered by Oligocene ignimbrites that define a reference surface from which to estimate late Cenozoic river incision. A 90-m-grid digital elevation model was used to characterize contemporary topography and interpolate the Late Oligocene surface of the ignimbrite plateau from a surface fit to the highest points in the relatively undissected uplands between major river valleys. Long-term river incision rates calculated from the difference between this reference surface and longitudinal profiles of 11 rivers that flow toward the Tepic-Zacoalco rift zone range from about 0.01 to 0.2 mm year^{-1}. River profiles of this region also show evidence of river capture driven by flexural uplift along the flank of the rift zone. River profile concavity values (θ) in the Sierra Madre Occidental range from 0.22 to 0.63, a range similar to that reported previously for a wide range of environments. In contrast, the empirically constrained ratio of exponents in the stream power model of river incision (m/n) ranges from 0.44 to 0.52, close to the expected theoretical value of 0.5. The wider range of observed θ values may illustrate how θ can differ from the driving values of m/n in non-steady-state bedrock river systems.

Keywords: Tectonic geomorphology; Ignimbrite plateau; River incision; Mexico

1. Introduction

In the last decade, renewed appreciation of the importance of bedrock river incision in landscape evolution has spurred research on the morphology and distribution of bedrock channels (e.g., Miller, 1991; Wohl, 1992b, 1998, 1999; Montgomery et al., 1996; Montgomery and Buffington, 1997; Montgomery and Gran, 2001; Tinkler and Wohl, 1998; Massong and Montgomery, 2000; Snyder et al., 2000). In addition, strong interest in feedback between erosion and rock uplift has focused attention on processes and rates of bedrock river incision (Seidl and Dietrich, 1992; Wohl, 1992a; Wohl et al., 1994; Seidl et al., 1994; Hancock et al., 1998; Pazzaglia et al., 1998; Pazzaglia and Brandon, 2001; Stock and Montgomery, 1999; Whipple et al., 1999, 2000; Kirby and Whipple, 2001). Isostatic response to river incision can focus rock uplift in areas of concentrated erosion (Beaumont et al., 1992; Willett et al., 1993; Zeitler et

* Corresponding author.
E-mail address: dave@ess.washington.edu (D.R. Montgomery).

0169-555X/03/$ - see front matter © 2003 Elsevier Science B.V. All rights reserved.
doi:10.1016/S0169-555X(03)00142-9

al., 1993, 2001; Finlayson et al., 2002), and landscape evolution models increasingly incorporate assumptions about rates of bedrock channel incision into studies linking fluvial geomorphology and tectonic processes (Tucker and Slingerland, 1994; Whipple and Tucker, 1999).

Rates of bedrock incision reflect both geophysical forcing and spatial variations in erosional processes, but little is known about how to calibrate quantitatively the characterization of the resistance of bedrock to these processes and, therefore, how to predict rates of bedrock river incision. Stock and Montgomery (1999) found a more than five-order-of-magnitude range in erosion resistance by modeling reported examples of long-term bedrock river incision with initial profiles of known age for a wide range of lithologies. Although the controlling variables are not easily distinguished, let alone quantified, erosion resistance scales the response time for evolution of bedrock river profiles (Whipple and Tucker, 1999; Whipple, 2001). Evaluations of bedrock erodibility typically back-calculate erosion resistance from single rivers and hence within region variability is less constrained than variability between regions.

Previous work on bedrock river incision has focused on tectonically active regions (typically convergent margin settings) with relatively little attention being given to rift zones and passive margins, although Young and McDougall (1993), Seidl et al. (1994), and Weissel and Seidl (1998) provide notable exceptions. But investigations of passive and extensional margins reveal that even in non-collisional settings erosion can strongly influence large-scale patterns of isostatic uplift (Gilchrist and Summerfield, 1990, 1991; Pazzaglia and Brandon, 1996). Of particular interest in the evolution of rifted margins is the fact that simulation modeling of flexural uplift along rift zones reveals the potential for drainage capture induced by margin upwarping (Tucker and Slingerland, 1994). Here we report results of a study of long-term river incision into Oligocene ignimbrites in the southern Sierra Madre Occidental, Mexico. In particular, we calculate long-term river incision rates into Tertiary ignimbrites in the western Mexican Volcanic Belt and discuss evidence for river capture due to flexural upwarping along the margin of the Tepic-Zacoalco rift zone.

2. Theory

Many workers report that channel slope varies as an inverse power law function of drainage area where

$$S = bA^{-\theta} \quad (1)$$

in which θ ranges from 0.2 to 1.0 (Hack, 1957; Flint, 1974; Tarboton et al., 1989; Moglen and Bras, 1995; Slingerland et al., 1998; Hurtrez et al., 1999; Snyder et al., 2000; Kirby and Whipple, 2001). For detachment-limited channel incision, modeling the local erosion rate (E) as a function of drainage area (A) and local slope (S) has become standard with

$$E = KA^m S^n \quad (2)$$

where K is a constant that incorporates climatic factors and bedrock erodibility, and m and n are thought to vary with different erosional processes (Kirkby, 1971). Eq. (2) can be rearranged to cast channel slope as a function of erosion rate, drainage area and bedrock resistance:

$$S = (E/K)^{(1/n)} A^{-(m/n)} \quad (3)$$

In the case of steady-state topography, in which E everywhere equals the local rock uplift rate U, Eq. (3) can be recast in terms of the local uplift rate such that

$$S = (U/K)^{(1/n)} A^{-(m/n)}, \quad (4)$$

allowing analysis of river profiles to yield information about the ratio of uplift (or bedrock incision) rates to bedrock erodibility (e.g., Hurtrez et al., 1999; Kirby and Whipple, 2001). Although Eqs. (1) and (4) imply that $\theta = m/n$ for steady-state topography, the relation of θ to m/n is not clear for nonequilibrium landscapes because of the potential effect of spatial and temporal variability in E and S along an evolving river profile. In addition, Roe et al. (2002) showed that feedback between orographically variable precipitation and discharge-driven river incision implies that $\theta \neq m/n$ for steady-state landscapes with strong orographic precipitation regimes.

3. Study area

The Sierra Madre Occidental of western Mexico, the world's largest Tertiary silicic province, consists of a Cretaceous granitic core covered by Oligocene ignimbrites (Fig. 1) (McDowell and Keizer, 1977; McDowell and Clabaugh, 1979; Albrecht and Goldstein, 2000; Henry and Aranda-Gomez, 2000). Ignimbrite deposition from 30 to 20 Ma predates onset of E–NE extension ca. 13 Ma (Fig. 2). The Sierra Madre Occidental is an excellent area to study long-term river incision because it is covered by an ignimbrite sheet that provides a reasonably well-constrained initial condition of known age, and a 3-arc-second digital elevation model (i.e., 90-m grid) is available for the region.

The Sierra Madre Occidental lies immediately north of the western Mexican Volcanic Belt, an active volcanic arc with substantial Pliocene to Holocene volcanism focused into a series of grabens and fault-bounded valleys (Righter, 1997). The southern end of the Sierra Madre Occidental is one of three large rift zones—the Tepic-Zacoalco, Colima, and Chapala rift zones—that intersect in western Mexico to form a

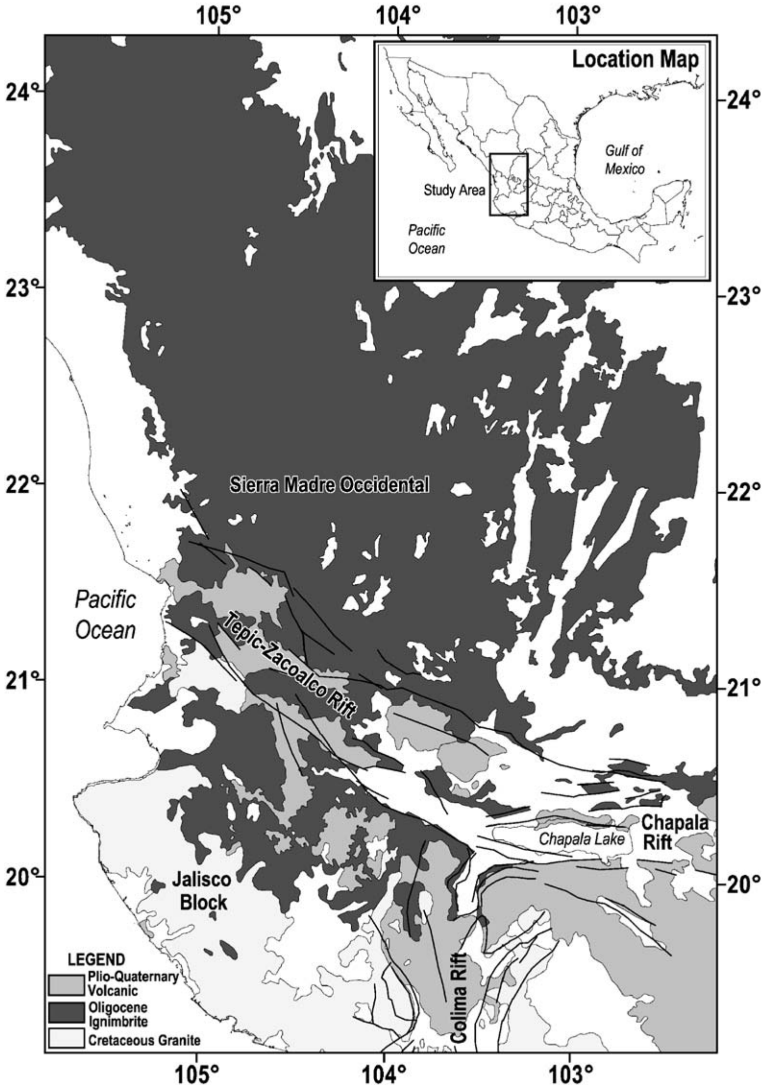

Fig. 1. Location of the study area southern Sierra Madre Occidental, Mexico. Note the presence of the Tepic-Zacoalco rift to the south.

structural triple junction that records the initiation of continental rifting (Luhr et al., 1985; Luhr, 1997; Allan et al., 1991). Onset of rifting is thought to be related to changes in offshore plate boundaries, in particular the migration of the East Pacific Rise onto the continent (Luhr et al., 1985; Allan et al., 1991) and possibly oblique subduction of the Rivera Plate (DeMets and Stein, 1990). The rifts are related to jumping of the Pacific–Rivera spreading ridge to the site of the Colima rift; four similar eastward ridge jumps have progressed northward in sequence along the East Pacific Rise during the last 12 Ma (Luhr, 1997).

Righter (1997) reported post-Pliocene bedrock incision rates of 0.23–0.25 mm year^{-1} in the Atenguillo River valley on the Jalisco block south of the Tepic-Zacoalco rift zone. We studied the longitudinal profiles of 11 rivers draining the southern Sierra Madre Occidental on the north side of the Tepic-Zacoalco rift (Table 1). These rivers rise in the relatively undissected uplands of the Sierra Madre Occidental and flow south through valleys incised into the ignimbrites and underlying rocks. Upon crossing into the Tepic-Zacoalco rift zone, the rivers join the Rio Santiago to flow westward and empty into the Pacific Ocean.

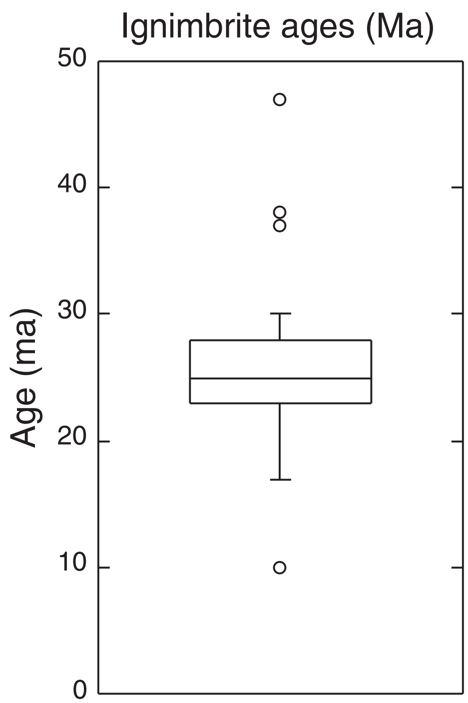

Fig. 2. Ignimbrite age distribution. Data compiled from Damon et al. (1979), Clark et al. (1981), Nieto-Obregón et al. (1981, 1985), Labarthe-Hernández et al. (1982), Lang et al. (1988), Castillo-Hernández and Romero-Rios (1991), Pasquaré et al. (1991), Moore et al. (1994), Webber et al. (1994), and Nieto-Samaniego et al. (1996, 1999).

Table 1
Morphometric characteristics of 11 rivers studied in the southern Sierra Madre Occidental

River	Name	Length (km)	Watershed area (km^2)	Maximun elevation (m.a.s.l.)	Minimun elevation (m.a.s.l.)
River 1	Bolaños	317	14,943	2379	426
River 2	Mango	241	8828	2900	390
River 3	Jesús María	176	4867	2724	217
River 4	Huajimic	55	573	1582	376
River 5	La Palmilla	35	400	2018	246
River 6	Camotlán	85	2053	2225	865
River 7	Joraviejo	56	629	2205	378
River 8	Chico	50	827	2232	557
River 9	Tlaltenango	167	3136	2568	1461
River 10	San Pedro	72	1706	2450	1627
River 11	Juchipila	289	7986	2387	949

4. Methods

We integrated a digital mosaic of 25 1° by 1° digital elevation model (DEM) files to create a single composite DEM of the southern Sierra Madre Occidental. The original source of this DEM, the GEMA DEM database (INEGI, 1994), covers all of Mexico at a grid resolution of 3-arc seconds (i.e., 90 m). The composite DEM forms an array extending from 101° to 106° W longitude and from 19° to 24° N latitude.

We analyzed 11 of the primary rivers in the study area (Fig. 3). Through on-screen digitizing using the afore mentioned DEM, we traced each river trajectory from its drainage divide to its confluence with the Rio Santiago, which bounds the study area to the south. We also traced the bounding drainage divides of both sides of each river basin. River trajectories were used to guide extraction of river profiles using a customized ARC/INFO macro (proffix2.aml) designed to address two major difficulties that plague efforts to extract river profiles from DEMs: (i) geographic projections are not equidistant, and (ii) river profiles generated from DEMs typically yield a bilinear inter-

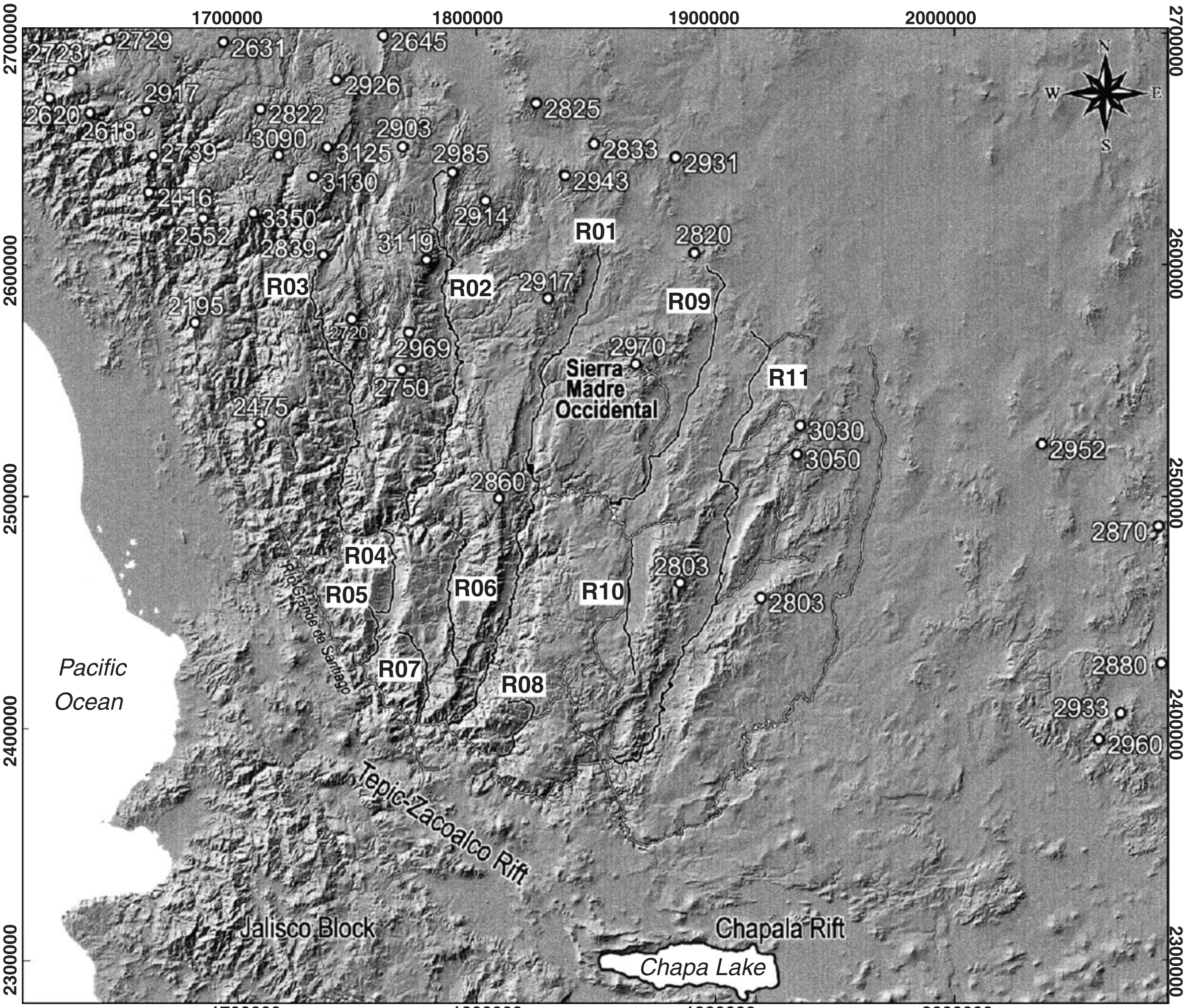

Fig. 3. Shaded relief digital elevation model of the southern Sierra Madre Occidental showing the river profile locations (R1 to R11) and high points used to estimate late-Oligocene topograpahy.

polation of the four lattice points nearest to the sample points and consequently can actually represent points partway up valley walls, especially along narrow bedrock valleys lacking substantial flood plains. In part due to this latter problem, DEMs frequently contain artificial "sinks" from which water cannot flow. Conventional river profile extraction algorithms treat these pits as artifacts that are filled to the elevation of their lowest outlet, or pour point. The usual solution is to flag the real sinks, such as lakes, and then fill the rest, resulting in a profile that has artificially flat zones composed of filled pits. But depending on the algorithm used in DEM creation, the initial lower-elevation values that get raised through pit filling routines may better record the actual river elevation.

The custom macro that we used accomodates different distance values for vertical, horizontal, and diagonal lines and preserves the lowest elevations along the represented stream bed rather than filling pits. Instead, when proffix2.aml encounters a filled sink, the program interrogates the raw DEM and traces the path of steepest descent. When it reaches a closed depression, it assigns weights to paths of shallowest ascent and to the direct path to the sink's pour point, from where it works its way uphill. When proffix2.aml reaches a part of the profile upstream of a filled section, it assigns a user-designated minimum slope to the formerly filled section of river. This results in a profile with neither flat spots nor closed depressions and yields a profile with a continuous downstream slope.

Using the modified river profiles, the contributing drainage area was calculated for each pixel along the river profiles. To reduce the effect of "noise" in the original DEM data as well as interpolation algorithms used to produce DEMs, we applied a smoothing function that averaged the river slope over 20 neighboring grid cells (10 up and 10 down the river profile) to obtain profiles that consistently dropped in elevation in the downstream direction without major discontinuities.

A representation of the "original" topography of the ignimbrite plateau was estimated from a surface fit to the 42 highest points in the study area using a smoothed quadratic interpolation. High points along the flank of the Tepic-Zacoalco rift were not considered in creating this reference surface to avoid bias because of the influence of local flexural uplift along the rift flank. The resulting surface has a slope of roughly 1° to the south and provides a reasonable interpretation of the depositional surface of the ignimbrite plateau.

Using the final delineation of the 11 river trajectories, we developed a raster map for each river trajectory and assigned each pixel an ordinal number in a downstream sequence from the drainage divide. Each river raster map was overlaid with both the original DEM and the estimated topography of the original ignimbrite plateau. We then generated a tabular data-

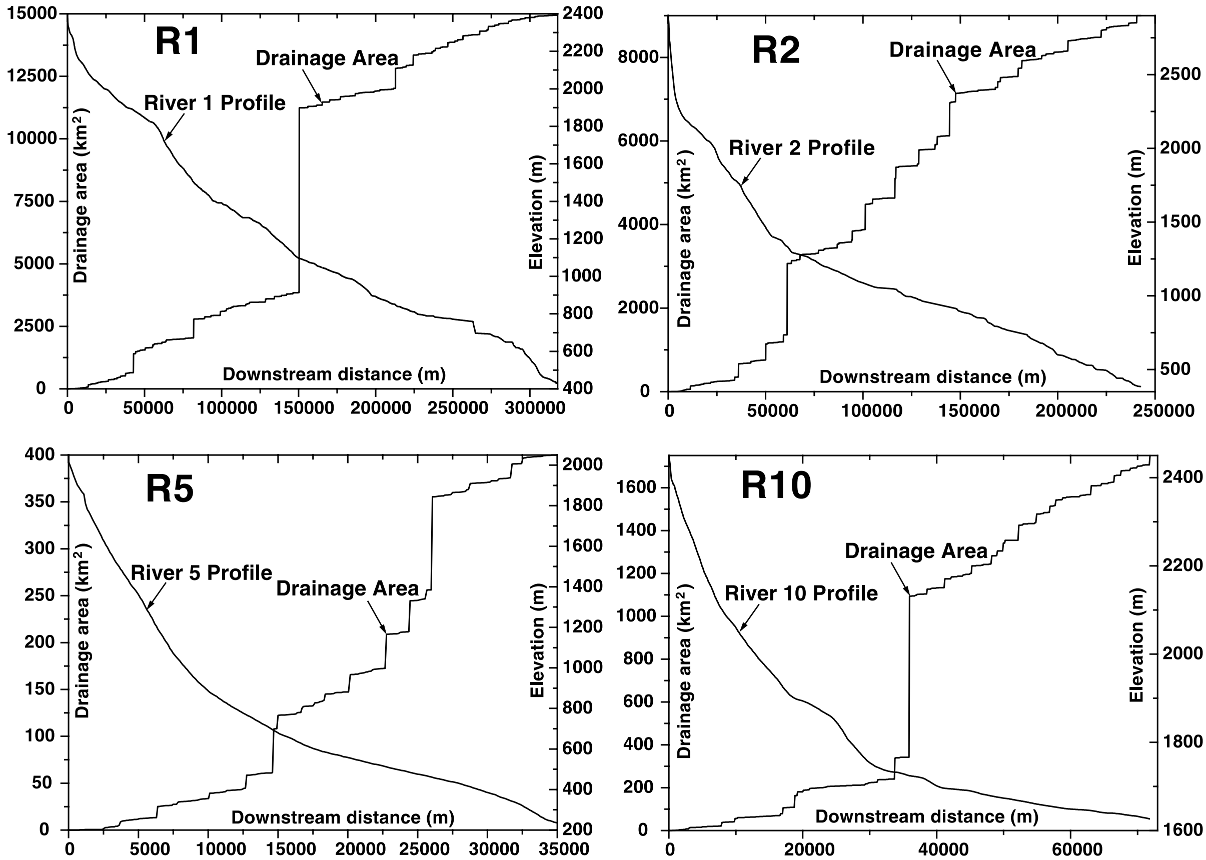

Fig. 4. Longitudinal profiles of several of the study rivers (R1, R2, R5, and R10).

base for each river trajectory containing the ordinal number for each pixel, its elevation value in the present topography DEM, and the elevation value in the ignimbrite plateau DEM. Total river incision was calculated for each grid cell by subtracting the present elevation from the interpolated original plateau elevation at each point along the river profile.

The age of the ignimbrites provides a limiting age on river incision. Although a river valley system carved into the Cretaceous basement likely existed at the time of ignimbrite eruption, any such valleys were most likely filled in by the massive deposition associated with emplacement of the ignimbrite sheets. Incision of the present valleys therefore post-dates ignimbrite deposition. Local long-term incision rates were estimated by dividing the net elevation difference between the inferred "original" elevation of the ignimbrite and the modern river elevation by the average ignimbrite age of 26 Ma to yield an average river incision rate. Estimates of the long-term incision rate under the assumption that all incision post-dates the 13 Ma onset of rifting would be double those estimated from the mean ignimbrite age.

5. Results

The form of river profiles in the study area ranges from smoothly concave to relatively linear and even convex in the lower reaches of some profiles (Fig. 4). The convex reaches presumably reflect either active subsidence of the Tepic-Zacoalco rift zone, or uplift

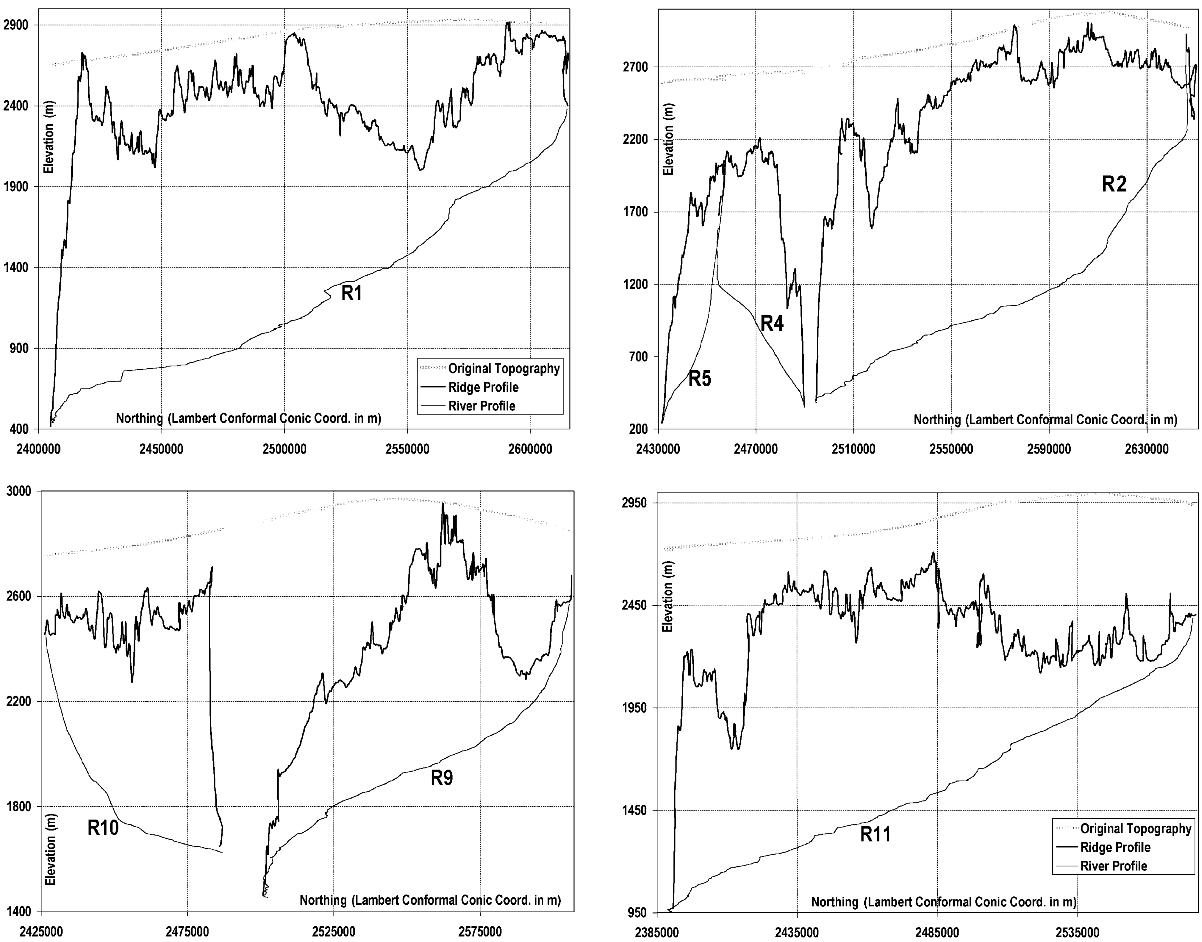

Fig. 5. Examples of river and ridge profiles illustrating the minimum estimates of post-Oligocene river incision versus distance along the river.

of the Sierra Madre Occidental. In addition, a number of rivers have distinct knickpoints midway along their profile. The knickpoints on rivers 1 and 2, however, are located just upstream of confluences with rivers 9 and 6, respectively, that initially drain away from the rift flank and flow north before turning east to join the rivers flowing in the neighboring valleys.

Long-term rates of river incision calculated by dividing the elevation difference between the present channel and the reconstructed ignimbrite plateau by 26 Ma (the mean ignimbrite age) increase downstream along each of the river profiles (Fig. 5). Hence, these rivers are not in steady-state. Long-term rates of bedrock incision along these profiles vary from about 0.01 to 0.1 mm year^{-1} assuming onset of incision at the mean ignimbrite age (26 Ma), or 0.02 to 0.2 mm year^{-1} assuming incision initiated coincident with rifting (13 Ma). Under either scenario, lower values in basin headwaters yield to progressively greater values farther down the river profile.

Plots of drainage area versus channel slope show the typical general inverse trend and wide scatter (Fig. 6). Power law regressions of drainage area versus slope for each river profile indicate θ values of 0.22 to 0.63 (Table 2). The wide range of R^2 values (0.19 to 0.85) indicates substantial variability to these relationships. Nonetheless, the rivers draining the southern Sierra Madre Occidental exhibit distinct relations between drainage area and slope in spite of the systematic variability in long-term erosion rates along their profiles.

Stratifying the individual drainage area–slope data points for each 20-grid-cell long reach from the profiles of all the study rivers into three ranges of long-term erosion rates of <0.03, 0.03–0.05, and

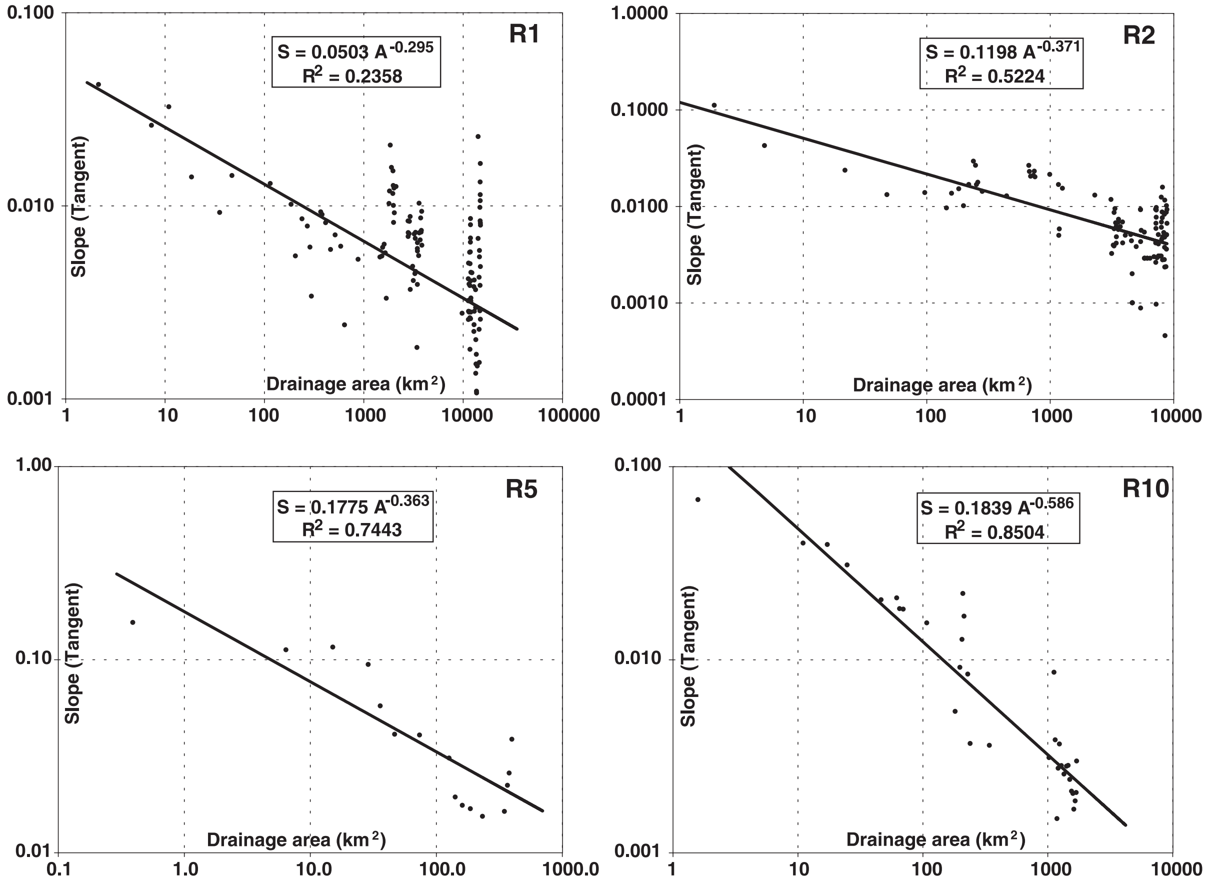

Fig. 6. Examples of slope versus area plots for several of the study rivers (R1, R2, R5, and R10).

Table 2
Power law relationships between drainage area and slopes ($S = cA^{-\theta}$) for the study rivers

River	Name	c	θ	R^2
River 1	Bolaños	0.05	0.30	0.24
River 2	Mango	0.12	0.37	0.52
River 3	Jesús María	0.29	0.55	0.63
River 4	Huajimic	0.06	0.22	0.35
River 5	La Palmilla	0.18	0.36	0.74
River 6	Camotlán	0.33	0.63	0.53
River 7	Joraviejo	0.10	0.26	0.42
River 8	Chico	0.10	0.25	0.53
River 9	Tlaltenango	0.04	0.32	0.35
River 10	San Pedro	0.18	0.59	0.85
River 11	Juchipila	0.04	0.32	0.19

>0.05 mm year^{-1} allows assessment of m/n and $(E/K)^{1/n}$ values based on the empirical relation between drainage area and slope for data from each erosion rate class. The exponents in power law regressions of these stratified data (Fig. 7) yield m/n values of 0.44 to 0.52, with R^2 values of 0.48 to 0.77 (Table 3). The variation in the coefficient, $(E/K)^{1/n}$, follows the variation in E between the three groups of data,

Table 3
Power law relationships between drainage area and slopes stratified by erosion rate for the points from the study rivers [$S = (E/K)^{(1/n)}A^{-(m/n)}$]

Erosion rate (mm year^{-1})	$(E/K)^{(1/n)}$	m/n	R^2	K[a] (m$^{0.5}$ year^{-1})
<0.03	0.11	0.52	0.77	2.7×10^{-7}
0.03–0.05	0.15	0.48	0.62	2.7×10^{-7}
>0.05	0.20	0.44	0.48	2.5×10^{-7}

[a] Assuming $n = 1$.

implying that K itself does not vary much in the relatively homogenous rocks of the study area. Assuming that $n = 1$ yields an estimated K of 2.5×10^{-7} m$^{0.5}$ year^{-1}.

6. Discussion

The association of distinct knickpoints just upstream of the confluences of small, initially north-draining rivers with south-draining rivers in neighboring valleys implies a history of river capture along the

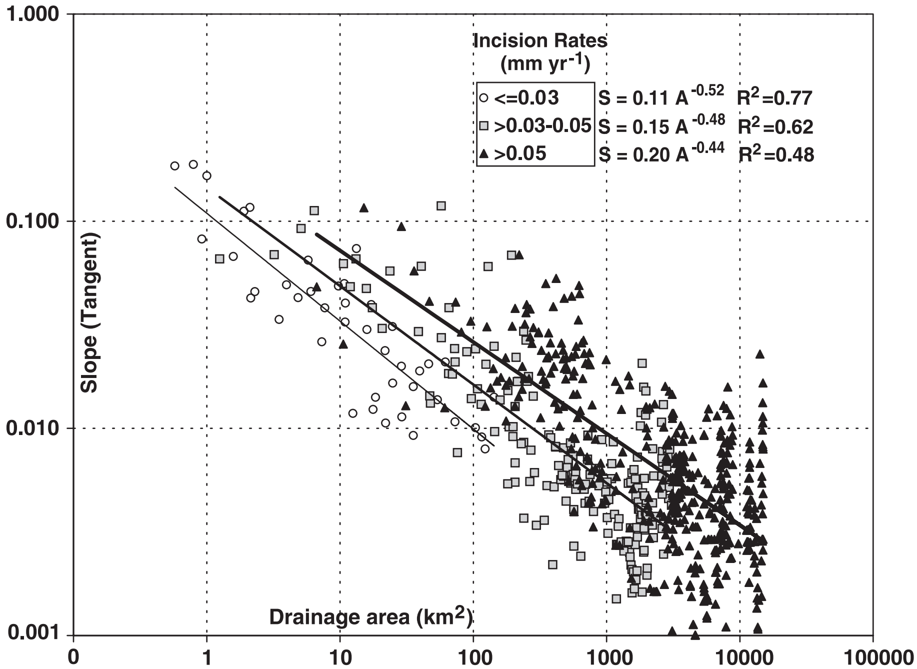

Fig. 7. Slope versus area data from all 11 rivers stratified by erosion rate determined as illustrated in Fig. 5. Power law regressions are for data within each grouping (Table 4).

northern flank of the Tepic-Zacoalco rift zone. Each of these north-flowing rivers shares a N–S oriented valley with a larger south-flowing river. In each case, N–S flowing rivers turn abruptly downstream of their confluence to drop through a narrow E–W trending gorge before merging with the river in the neighboring valley. We suspect that these short north-flowing rivers reflect flexural uplift of the margin of the Tepic-Zacoalco rift zone that was sufficient to reverse the course of these rivers, and trigger their diversion and capture by overtopping their lateral drainage divide. The apparent reversal, diversion, and capture of these rivers is in accord with the predictions of Tucker and Slingerland's (1994) surface process model simulations of river-system evolution on rifted margins.

Although substantial variability in the combined datasets exists, the K values are lower than those reported by Stock and Montgomery (1999) for other areas with volcaniclastic rocks, and are more similar to values they report for more lithified granitoids and meta-sediments. The rates of long-term river incision indicated by our analysis are comparable to rates reported by other researchers for long-term river incision in extensional settings or volcanic islands (Table 4). However, our rates are lower than those reported by Righter (1997) for channels on the Jalisco Block on the opposite side of the Tepic-Zacoalco rift. As Righter's (1997) rates were based on post-Pliocene incision, this difference could be due to either acceleration of bedrock incision in the Pleistocene, differences in erodibility in the two areas on either side of the rift zone, or because the ignimbrite ages only provide limiting ages on the onset of river incision in the Sierra Madre Occidental and, therefore, minimum incision rates for the period of active river incision. If the incision of the Sierra Madre Occidental river valleys commenced at 13 Ma coincident with the onset of rifting, then the incision rates reported here would double, bringing the upper end of the range of incision rates into general agreement with those reported by Righter (1997). While the K values inferred from Fig. 7 are also sensitive to the time scale over which river incision is assumed to have been effective, the range of 13–26 Ma yields calculated river incision rates of 0.01–0.2 mm year^{-1}.

Table 4
Comparison of incision rates between the southern Sierra Madre Occidental and other areas

Locality	Tectonic characteristics	Incision rate (mm year^{-1})[a]	Reference
Southern Sierra Madre Occidental	Oligocene ignimbritic plateau	0.01–0.2	This study
Atenguillo River	Plio-Quaternary extension	0.23–0.25	Righter et al. (1995) and Righter (1997)
Grand Canyon	Plio-Quaternary extension	0.09–0.11	Damon et al. (1974)
Utah	Plio-Quaternary extension	0.30	Hamblin et al. (1981)
Rio Grande Rift	Plio-Quaternary extension	< 0.01–0.08	Grimm (1982)
Israel	Extension	0.10	Wohl et al. (1994)
Hawaii	Ocean islands	< 0.01–0.08	Seidl et al. (1994)

[a] Assuming incision commenced 13–26 Ma, as constrained by onset of rifting (13 Ma) and mean ignimbrite age (26 Ma).

The m/n values of 0.42 to 0.52 determined by analysis of data grouped into locations with similar post-Oligocene erosion rates are similar to those expected based on models for river incision driven by unit stream power and are not dependent on the time scale over which incision is assumed to have occurred. Neither are they dependent on the steady-state assumption, as local values of E are known independently from the long-term incision of the ignimbrite plateau. The empirically derived θ values of 0.22 to 0.63 based on slope–area relations for individual rivers span much of the range of values reported in previous studies of rivers in other regions, suggesting that much of the range in previously observed θ values may simply reflect that some of the rivers in question do not have steady state profiles and that $\theta \neq m/n$ for these non-steady-state rivers.

7. Conclusions

Ignimbrite sheets, such as the southern Sierra Madre Occidental, provide ideal locations for studying long-term river incision because of their relatively simple initial condition as a depositional surface and their amenability to conventional radiometric dating. The long-term bedrock river incision rates of 0.01–0.2 mm year^{-1} determined for the southern Sierra Madre Occidental are comparable to rates reported for a variety of extensional and volcanic landscapes suggesting that such rates may be typical for rifted margin settings. Although the wide range of river concavity (i.e., θ) values for the southern Sierra Madre Occidental spans the range of values reported previously, much of the variability in our data likely is due to the non-steady-state nature of the river profiles. This supposition is supported by the finding that the m/n values determined by normalizing for differences in bedrock lowering rates are consistent with values predicted by conventional models of river incision. The non-steady-state nature of these river profiles appears to impart a wider range in θ than is apparent in empirically estimated m/n values that describe the integrated effect of erosional processes.

Acknowledgements

We thank Harvey Greenberg for developing the ARC/INFO macro proffix2.aml and for assistance with GIS analyses. This research was funded in part by CONACYT and DGAPA-UNAM, México.

References

Albrecht, A., Goldstein, S., 2000. Effects of basement composition and age on silicic magmas across an accreted terrane–Precambrian crust boundary, Sierra Madre Occidental, Mexico. Journal of South American Earth Sciences 13, 255–273.

Allan, J.F., Nelson, S.A., Luhr, J.F., Carmichael, I.S.E., Wopat, M., Wallace, P.J., 1991. Pliocene–recent rifting in SW Mexico and associated volcanism: an exotic terrane in the making. In: Dauphin, J.P., Simoneit, B.R.T. (Eds.), The Gulf and Peninsular Province of the Californias. American Association of Petroleum Geology Memoir, vol. 47, pp. 425–445. Tulsa, OK.

Beaumont, C., Fullsack, P., Hamilton, J., 1992. Erosional control of active compressional orogens. In: McClay, K.R. (Ed.), Thrust Tectonics. Chapman & Hall, New York, pp. 1–18.

Castillo-Hernández, D., Romero-Rios, F., 1991. Estudio geológico-regional de Los Altos, Jalisco y El Bajío. Comisión Federal de Electricidad, Gerencia de Proyectos Geotermoeléctricos. Depto. Exploración, Open File Report 02-91, Mexico City. 35 pp.

Clark, K.F., Damon, P.E., Shafiquillah, M., Ponce, B.F., Cárdenas, D., 1981. Sección geológica-estructural a través de la parte Sur de la Sierra Madre Occidental, entre Fresnillo y la costa de Nayarit. Asoc. Ingenieros Mineros, Metalúrgicos y Geólogos de México. Memoria Técnica XIV, 69–99.

Damon, P.E., Shafiqullah, M., Leventhal, J.S., 1974. K–Ar chronology for the San Francisco Volcanic Field and rate of erosion of the Little Colorado River. In: Karlstrom, T.N.V., Swann, G.A., Eastwood, R.L. (Eds.), Geology of Northern Arizona with Notes on Archeology and Paleoclimate: Part I. Regional Studies. Geological Society of America 27th Annual Meeting, Rocky Mountain Section, Flagstaff, AZ., pp. 221–235.

Damon, P.E., Nieto, O.J., Delgado, A.L., 1979. Un plegamiento neogénico en Nayarit y Jalisco y evolución geomórfica del Río Grande de Santiago. Asoc. Ingenieros Mineros, Metalúrgicos y Geólogos de México. Memoria Técnica XXIII, 156–191.

DeMets, C., Stein, S., 1990. Present day kinematics of the Rivera Plate and implications for tectonics in southwestern Mexico. Journal of Geophysical Research 95, 21931–21948.

Finlayson, D.P., Montgomery, D.R., Hallet, B., 2002. Spatial coincidence of rapid inferred erosion with young metamorphic massifs in the Himalayas. Geology 30, 219–222.

Flint, J.J., 1974. Stream gradient as a function of order, magnitude, and discharge. Water Resources Research 10, 969–973.

Gilchrist, A.R., Summerfield, M.A., 1990. Differential denudation and flexural isostasy in formation of rifted-margin upwarps. Nature 346, 739–742.

Gilchrist, A.R., Summerfield, M.A., 1991. Denudation, isostasy and landscape evolution. Earth Surface Processes and Landforms 16, 555–562.

Grimm, J.P., 1982. Base level changes and incision rates for canyons draining the Mount Taylor Volcanic field, New Mexico. In: Wells, S.G., Grambling, J.A., Callender, J.F. (Eds.), Albuquerque Country II. Guidebook, vol. 33. New Mexico Geological Society, Albuquerque, NM, pp. 60–61.

Hack, J.T., 1957. Studies of longitudinal stream profiles in Virginia and Maryland. United States Geological Survey Professional Paper 294-B. Washington, DC, 97 pp.

Hamblin, W.K., Damon, P.E., Bull, W.B., 1981. Estimates of vertical crustal strain rates along the western margins of the Colorado Plateau. Geology 9, 293–298.

Hancock, G.S., Anderson, R.S., Whipple, K.X., 1998. Beyond power: bedrock river incision process and form. In: Tinkler, K., Wohl, E. (Eds.), Rivers Over Rock: Fluvial Processes in Bedrock Channels. Geophysical Monograph, vol. 107. American Geophysical Union, Washington, DC, pp. 35–60.

Henry, C.D., Aranda-Gomez, J.J., 2000. Plate interactions control middle–late Miocene, proto-Gulf and Basin and Range extension in the southern basin and Range. Tectonophysics 318, 1–26.

Hurtrez, J.-E., Lucazeau, F., Lavé, J., Avouac, J.-P., 1999. Investigation of the relationships between basin morphology, tectonic uplift, and denudation from the study of an active fold belt in the Siwalik Hills, central Nepal. Journal of Geophysical Research 104, 12796–12799.

INEGI, 1994. GEMA (Geomodelos de Altimetría del Territorio Nacional). Instituto Nacional de Estadística Geografía e Informática. Compact Disc with 255 1° by 1° DEM files from topographic mapas at 1,250,000 scale. ISBN: 970-13-0474-8.

Kirby, E., Whipple, K., 2001. Quantifying differential rock-uplift rates via stream profile analysis. Geology 29, 415–418.

Kirkby, M.J., 1971. Hillslope process-response models based on the continuity equation. In: Brunsden, D. (Ed.), Slopes: Form and Process, vol. 3. Institute of British Geographers Special Publication, London, pp. 15–30.

Labarthe-Hernández, G., Tristán-González, M., Aranda-Gómez, J.J., 1982. Revisión Estratigráfica del Cenozoico de la Parte Central del Estado de San Luis Potosí. Universidad Autónoma de San Luis Postosí, Instituto Geología, Folleto técnico #85, Mexico City. 208 pp.

Lang, B., Steinitz, G., Sawkins, F.J., Simmons, S.F., 1988. K–Ar age studies in the Fresnillo Silver District, Zacatecas, Mexico. Economic Geology 83, 1642–1646.

Luhr, J.F., 1997. Extensional tectonics and the diverse primitive volcanic rocks in the Western Mexican Volcanic Belt. The Canadian Mineralogist 35, 473–500.

Luhr, J.F., Nelson, S.A., Allan, J.F., Carmichael, I.S.E., 1985. Active rifting in southwestern Mexico: manifestations of an incipient eastward spreading ridge jump. Geology 13, 54–57.

Massong, T.M., Montgomery, D.R., 2000. Influence of lithology, sediment supply, and wood debris on the distribution of bedrock and alluvial channels. Geological Society of America Bulletin 112, 591–599.

McDowell, F.W., Clabaugh, S.E., 1979. Ignimbrites of the Sierra Madre Occidental and their relation to the tectonic history of western Mexico. In: Chapin, C.E., Elston, W.E. (Eds.), Ash-Flow Tuffs, vol. 180. Geological Society of America Special Paper, Boulder, CO, pp. 113–124.

McDowell, F.W., Keizer, R.P., 1977. Timing of mid-Tertiary volcanism in the Sierra Madre Occidental between Durango City and Mazatlan, Mexico. Geological Society of America Bulletin 88, 1479–1487.

Miller, J.R., 1991. Controls on channel form along bedrock-influenced alluvial streams in south-central Indiana. Physical Geography 12, 167–186.

Moglen, G.E., Bras, R.L., 1995. The effect of spatial heterogeneities on geomorphic expression in a model of basin evolution. Water Resources Research 31, 2613–2623.

Montgomery, D.R., Buffington, J.M., 1997. Channel reach morphology in mountain drainage basins. Geological Society of America Bulletin 109, 596–611.

Montgomery, D.R., Gran, K.B., 2001. Downstream variations in the width of bedrock channels. Water Resources Research 37, 1841–1846.

Montgomery, D.R., Abbe, T.B., Peterson, N.P., Buffington, J.M., Schmidt, K.M., Stock, J.D., 1996. Distribution of bedrock and alluvial channels in forested mountain drainage basins. Nature 381, 587–589.

Moore, G., Marone, C., Carmichael, I.S.E., Renne, P., 1994. Basaltic volcanism and extension near the intersection of the Sierra Madre volcanic province and the Mexican Volcanic Belt. Geological Society of America Bulletin 106, 383–394.

Nieto-Obregón, J., Delgado-Argote, I., Damon, P.E., 1981. Relaciones petrológicas y geocronológicas del magmatismo de la Sierra Madre Occidental y el Eje Neovolcánico en Nayarit, Jalisco y Zacatecas Asoc. Ingenieros Mineros, Metalúrgicos y Geólogos de México. Memoria Técnica XIV, 327–361.

Nieto-Obregón, J., Delgado-Argote, I., Damon, P.E., 1985. Geochronologic, petrologic and structural data related to large morphologic features between the Sierra Madre Occidental and the Mexican Volcanic Belt. Geofísica Internacional 24, 623–663.

Nieto-Samaniego, A.F., Macias-Romo, C., Alaniz-Alvarez, S.A., 1996. Nuevas edades isotópicas de la cubierta volcánica cenozoica de la parte meridional de la Mesa Central, México. Revista Mexicana de Ciencias Geológicas 13, 117–122.

Nieto-Samaniego, A.F., Ferrari, L., Alaniz-Alvarez, S.A., Labarthe-Hernández, G., Rosas-Elguera, J., 1999. Variation of Cenozoic extension and volcanism across the southern Sierra Madre Occidental volcanic province, Mexico. Geological Society of America Bulletin 111, 347–363.

Pasquaré, G., Ferrari, L., Garduño, V.H., Tibaldi, A., Vezzoli, L., 1991. Geologic Map of the Central Sector of the Mexican Volcanic Belt, States of Guanajuato and Michoacan, Mexico. Geological Society of America, Map and Chart Series MCH 072, 1 sheet. 21 pp.

Pazzaglia, F.J., Brandon, M.T., 1996. Macrogeomorphic evolution of the post-Triassic Appalachian mountains determined by deconvolution of the offshore basin sedimentary record. Basin Research 8, 255–278.

Pazzaglia, F.J., Brandon, M.T., 2001. A fluvial record of long-term steady-state uplift and erosion across the Cascadia forearc high, western Washington State. American Journal of Science 300, 385–431.

Pazzaglia, F.J., Gardner, T.W., Merritts, D.J., 1998. Bedrock fluvial incision and longitudinal profile development over geologic time scales determined by fluvial terraces. In: Tinkler, T.J., Wohl, E.E. (Eds.), Rivers Over Rock: Fluvial Processes in Bedrock Channels. American Geophysical Union Geophysical Mongraph, vol. 107, pp. 207–236.

Righter, K., 1997. High bedrock incision rates in the Atenguillo River Valley, Jalico, western Mexico. Earth Surface Processes and Landforms 22, 337–343.

Righter, K., Carmichael, I.S.E., Becker, T.A., Renne, R.P., 1995. Pliocene to Quaternary volcanism and faulting at the intersection of the Gulf of California and the Mexican Volcanic Belt. Geological Society of America Bulletin 107, 612–626.

Roe, G., Montgomery, D.R., Hallet, B., 2002. Effects of orographic precipitation variations on steady-state river profiles. Geology 30, 143–146.

Seidl, M.A., Dietrich, W.E., 1992. The problem of channel erosion into bedrock. In: Schmidt, K.-H., dePloey, J. (Eds.), Functional Geomorphology: Landform Analysis and Modelling. Catena Supplement, vol. 23, pp. 101–124.

Seidl, M.A., Dietrich, W.E., Kirschner, J.W., 1994. Longitudinal profile development into bedrock: an analysis of Hawaiian channels. Journal of Geology 102, 457–474.

Slingerland, R., Willett, S.D., Hovius, N., 1998. Slope–area scaling as a test of fluvial bedrock erosion laws. EOS, Transactions of the American Geophysical Union 79, F358 (Fall Meet. Suppl.).

Snyder, N.P., Whipple, K.X., Tucker, G.E., Merritts, D.J., 2000. Landscape response to tectonic forcing: digital elevation model analysis of stream profiles in the Mendocino triple junction region, northern California. Geological Society of America Bulletin 112, 1250–1263.

Stock, J.D., Montgomery, D.R., 1999. Geologic constraints on bedrock river incision using the stream power law. Journal of Geophysical Research 104, 4983–4993.

Tarboton, D.G., Bras, R.L., Rodriguez-Iturbe, I., 1989. Scaling and elevation in river networks. Water Resources Research 25, 2037–2051.

Tinkler, K., Wohl, E., 1998. A primer on bedrock channels. In: Tinkler, K.J., Wohl, E.E. (Eds.), Rivers Over Rock: Fluvial Processes in Bedrock Channels. Geophysical Monograph, vol. 107. American Geophysical Union, Washington, DC, pp. 1–18.

Tucker, G.E., Slingerland, R.L., 1994. Erosional dynamics, flexural isostasy, and long-lived escarpments: a numerical modeling study. Journal of Geophysical Research 99, 12229–12243.

Webber, K.L., Fernández, L.A., Simmons, B., 1994. Geochemistry and mineralogy of the Eocene–Oligocene volcanic sequence, southern Sierra Madre Occidental, Juchipila, Zacatecas, Mexico. Geofísica Internacional 33, 77–89.

Weissel, J.K., Seidl, M.A., 1998. Inland propagation of erosional escarpments and river profile evolution across the southeast Australian passive continental margin. In: Tinkler, K.J., Wohl, E.E. (Eds.), Rivers Over Rock: Fluvial Processes in Bedrock Channels. Geophysical Monograph, vol. 107. American Geophysical Union, Washington, DC, pp. 189–206.

Whipple, K.X., 2001. Fluvial landsacpe response time: how plausible is steady-state denudation? American Journal of Science 301, 313–325.

Whipple, K.X., Tucker, G.E., 1999. Dynamics of the stream-power river incision model: implications for height limits of mountain ranges, landscape response time scales, and research needs. Journal of Geophysical Research 104, 17661–17674.

Whipple, K.X., Kirby, E., Brocklehurst, S.H., 1999. Geomorphic limits to climate-induced increases in topographic relief. Nature 401, 39–43.

Whipple, K.X., Hancock, G.S., Anderson, R.S., 2000. River incision into bedrock: mechanics and relative efficacy of plucking, abrasion, and cavitation. Geological Society of America Bulletin 112, 490–503.

Willett, S., Beaumont, C., Fullsack, P., 1993. Mechanical model for the tectonics of doubly vergent compressional orogens. Geology 21, 371–374.

Wohl, E.E., 1992a. Gradient irregularity in the Herbert Gorge of northeastern Australia. Earth Surface Processes and Landforms 17, 69–84.

Wohl, E.E., 1992b. Bedrock benches and boulder bars: floods in the Burdekin Gorge of Australia. Geological Society of America Bulletin 104, 770–778.

Wohl, E.E., 1998. Bedrock channel morphology in relation to erosional processes. In: Tinkler, K.J., Wohl, E.E. (Eds.), Rivers Over Rock: Fluvial Processes in Bedrock Channels. Geophysical Monograph, vol. 107. American Geophysical Union, Washington, DC, pp. 133–151.

Wohl, E.E., 1999. Incised bedrock channels. In: Darby, S.E., Simon, A. (Eds.), Incised River Channels. Wiley, New York, pp. 187–217.

Wohl, E.E., Greenbaum, N., Schick, A.P., Baker, V.R., 1994. Controls on bedrock channel incision along Nahal Paran, Israel. Earth Surface Processes and Landforms 19, 1–13.

Young, R., McDougall, I., 1993. Long-term landscape evolution: early Miocene and modern rivers in southern New South Wales, Australia. Journal of Geology 101, 35–49.

Zeitler, P.K., Chamberlain, C.P., Smith, H.A., 1993. Synchronous anatexis, metamorphism, and rapid denudation at Nanga Parbat (Pakistan Himalaya). Geology 21, 347–350.

Zeitler, P.K., et al., 2001. Erosion, Himalayan geodynamics, and the geomorphology of metamorphism. GSA Today 11, 4–9.